UDK: 621.453/457.001.57:519.637
COSATI: 19-07, 16-04, 16-02

Enhancing the Precision of Artillery Rockets Using Pulsejet Control Systems with Active Damping

Bojan Pavković[1)]
Miloš Pavić[1)]
Danilo Ćuk[2)]

Long- and medium-range artillery rockets are used for indirect fire on distant targets. As they have large impact point dispersion, they are considered to be area weapons and are fired from multi tube launchers. Achieving high hit probability requires spending a vast number of rockets. A control system application enables the reduction of their impact point dispersion and the increase of hit probability. Pulsejet control systems are simple, inexpensive and efficient enough to achieve the dispersion reduction which justifies their application. This paper presents a simplified control scheme for artillery rockets named the active damping method which performs a correction of disturbances immediately after a rocket exits a launcher tube. It is shown that the application of such a control system achieves a significant dispersion reduction, and that it stands as an efficient method for the reduction of the effect of all disturbances except the deviation of the rocket motor total impulse.

Key words: **rocket artillery, multi tube rocket launcher, rocket projectile, rocket control, rocket guidance, control system, pulse jet control, precision, error correction, impact point dispersion, effect on the target, Monte Carlo method.**

Nomenclature

I_c, N-s – single jet impulse
I_{tot}, kN-s – total impulse of the main rocket motor
J_y, kg-m^2 – transversal moment of inertia
K – command coefficient
K_P – control system gain
K_ω – feedback constant
$\mathbf{L}_{\tilde{B}B}$ – transformation matrix
l_I, m – distance of pulse jets from the C.G.
m_q, 1/s – dynamic derivative
m_w, m^{-1}s^{-1} – dynamic derivative
N_I – number of pulse jets
p, q, r, rad/s – angular rate components
t, s – time
$t_{\min}$, s – minimum time between two consecutive pulses
V, m/s – velocity of the rocket
V_{Wx}, V_{Wy} – side wind velocity
w, u – velocity projections on the z and x axes
x_f, m – range
z_w, 1/s – dynamic derivative
α, rad – angle of attack
ε, mrad – trust misalignment angle
ε_Φ, rad – pulse activation threshold
Φ, Θ, Ψ, rad – roll, pitch and yaw angles
Φ_d, rad – activation delay
$\Delta\Phi_n$, rad – pulsejet roll angle
Φ_ω, rad – command angle
τ_I, s – pulse duration
$\boldsymbol{\omega}$, rad/s – angular rate vector
ω_n, rad/s – natural frequency
$\boldsymbol{\omega}_{yz}$, rad/s – angular rate vector in the Cyz plane
ζ_n – damping ratio

Subscripts

AD – active damping
c – control values
R – reference value
0 – values at the launcher exit

Superscripts

~ – values in the aero-ballistic frame

Introduction

ARTILLERY rockets are used in battlefields for indirect fire on distant targets. As the line of sight is not available, aiming is performed on the basis of known coordinates of the launcher and the target. In order to achieve a long range, the launching is performed at high elevation angles. A long range, low initial velocity and long duration of flight make these rockets very sensitive to the

[1)] Military Technical Institute (VTI), Ratka Resanovića 1, 11132 Belgrade, SERBIA
[2)] University of Belgrade, Faculty of Mechanical Engineering, Kraljice Marije 16, 11120 Belgrade, SERBIA

influence of disturbances on their hit precision. Increasing the range reduces the precision of artillery rocket systems. Therefore, they are commonly used as area weapons rather than precision ones. The efficient covering of a targeted area requires a large number of rockets launched from multi-tube launchers. This scenario for artillery rockets finds its place in modern warfare due to many advantages over the classic artillery, which are: longer range, high fire power concentration in a short period of time, low launcher price and its high mobility. On the other hand, rockets have a higher price than classic artillery shells, and their precision is lower.

Modern warfare, however, demands higher precision in order to avoid or reduce the collateral damage as much as possible. In addition, there is a requirement for an increased maximum range in order to gain the tactical advantage. These two demands are contradictory, as the increase of the range deteriorates the precision. On the other hand, a reduction of weapons cost is required. In the case of artillery rockets, these demands could be met by an increase of their precision and a reduction of the number of rockets needed for target destruction. All these demands can be achieved using guided artillery rockets, or rockets with enhanced precision. The applied control systems, in these cases, are required to achieve a dispersion reduction which economically justifies their application.

Applying control systems on artillery rockets launched from multi-tube launchers demands the optimization of their cost, which should correspond to the reduction of the number of rockets needed for target destruction. Low cost control systems can be achieved using pulsejets. Such executive organs consist of a certain number of small rocket motors, placed on a control ring in the front section of the rocket. Besides having no moving parts, pulsejet control systems have very low energy consumption and use very simple electronics for the activation of control jets. Their reliability and cost are very advantageous.

Simplified control systems have been considered recently in a number of scientific papers for the application on rockets as well as for other types of smart ammunition. Continuous research and development of micro-electro-mechanical sensors (MEMS) allows the implementation of complete sensor systems on low and medium caliber projectiles. Significant efforts in the field of control mechanisms have brought new and innovative solutions. The considered concepts are pulsejets [1-6], synthetic jets [7], drag brakes [8,9], deployable pins [10,11], moveable nose [12], moveable canards [13], dual-spin projectiles [14,15], ram air deflection [16], and internal translating mass [17].

The pulsejet application on rockets has been originally considered by Harkins and Brown [1]. They have proposed active damping as a dispersion reduction method for 2.75 in direct fire air to surface rockets, fired from multi tube launchers. Jitpraphai and Costello [2] have proposed (also for direct fire rockets) a simplified control system with pulsejets and the window-based trajectory tracking control law. Jitpraphai, Burchett and Costello [3] have given a comparison of different guidance laws in the case of direct fire rockets and pulsejet control mechanisms. They have compared window-based trajectory tracking (TT), parabolic and proportional navigation (PAPNG) and classic proportional navigation (PN). Gupta, Saxena, Singhal and Ghosh [4] have extended the study [2] to artillery rockets fired at low elevations, in which case there is no significant difference between artillery and direct fire rockets. Fired at high elevations, artillery rockets have a highly curved and long trajectory and fly through different atmospheric conditions, which makes the use of previously described control laws inefficient. Pavković, Ćuk and Pavić [5] have suggested a guidance law named the trajectory tracking with pulse frequency modulation (TT with PFM) which forms a control signal based on rocket deviation from the reference trajectory and transforms it into an array of pulses using pulse frequency modulation. Such a control system is applicable on artillery rockets fired at high elevations. Ćuk, Pavić and Pavković [6] have given a comparison of different guidance laws for mortar shells with pulsejet control mechanisms. Mandić [18] has given an algorithm with the flight path angle control, regardless of the used control system. The subject of this paper is the application of the active damping method for the precision enhancing of artillery rockets.

The Active Damping Method

The basis for this correction method was given by Harkins and Brown [1], who have considered 2.75 in direct fire air to surface rockets, fired from multi tube launchers. They have suggested a simplified control system, based on pulsejets and rate gyroscopes as feedback sensors. By the application of such a control system, they have managed to reduce the impact point dispersion by the factor of 4. In that case, the deviations of the pitch and yaw rates at the launcher exit had a much more dominant influence on the impact point dispersion than the deviation of the rocket motor total impulse.

In the case of artillery rockets, the situation is significantly different. The total impulse deviation is by far the most important factor for the impact point dispersion. However, a situation could be different again. The total impulse of the main rocket motor is the parameter controlled through the production process as the amount of rocket propellants. Various methods, such as the production of the charge in segments and their pairing as well as the division of the produced rockets in different weight classes could produce a significant reduction in total impulse deviation within a single production batch. The uniformity of the propellant chemical composition could also be improved by using advanced production control methods as well as by using large mixers for the production of propellant for a large number of rockets. Further improvement in the propellant uniformity can be achieved by control of the produced propellant's characteristics for each batch. On the other hand, thrust optimization for range maximization could result in the burn phase prolongation and the reduction of launcher exit velocity, thus increasing the pitch rate and its deviation. Therefore, in the case of a high quality production and thrust optimization with respect to the range increase, it is possible for the total impulse deviation to lose its domination in the impact point dispersion, and for the active damping method to find its use in artillery rockets.

Gantmakher and Levin [19] have given a detailed analysis of the impact point dispersion of artillery rockets, showing that that the disturbances occurring immediately after the launcher exit have the greatest effect. The angle of attack appearing in that period is the effect of the initial oscillations of pitch and yaw rates, wind and thrust misalignment. The task of the active damping control system is to bring the pitch and yaw rates in the period immediately after launch to some specified values and to

suppress their oscillations. Since this task does not require much energy and since the control process is performed immediately after launch when the rocket velocity is low, it is logical to use a pulsejet control system. Such control systems are characterized by a low price and complexity, absence of moving parts, high reliability and efficiency even in the case of low rocket velocities. These facts make them acceptable for implementation even on artillery rockets with smaller caliber and range.

The main tool for the following analysis is a simulation of the mathematical model of rocket flight with 6 degrees of freedom (6-DOF), given in [20]. The rocket configuration used in the simulation study is a representative long-range 262 mm artillery rocket, 4.7 m long, fin-stabilized, with four pop-out fins on its rear part. The lateral pulsejet ring is located at 0.4 m from the nose tip of the rocket. The main rocket motor burns for 20 s and imparts an impulse to the rocket of I_{tot} = 33.4 kN-s. The thrust is divided into two phases: 6000 daN for the first 0.76 s and 1500 daN for the rest of the burn phase. The rocket weight, the mass center location from the nose tip, the axial and transversal moments of inertia before and after burn are 390/225 kg, 2.65/2.47 m, 3.45/2.15 kg-m^2, and 563/447 kg-m^2, respectively. Nominally, the rocket exits the launcher at V_0 = 41.7 m/s and p_0 = 33 rad/s. The exit roll rate is achieved by the rifled launching tube. A case with the range of x_f = 49900 m, which is less that the maximum one, is analyzed. The initial values of the system states and their statistics are given in Table 1. It is assumed that all random values are Gaussian.

Table 1. Reference and disturbance values

Parameter	Reference value	Standard deviation
q_0 [rad/s]	-0.099	-0.042
r_0 [rad/s]	0	0.021
Θ_0 [deg]	58.6	0.03
Ψ_0 [deg]	0.23	0.018
V_{Wx} [m/s]	0	2
V_{Wy} [m/s]	0	2
I_{tot} [%]	100	0.5
ε [mrad]	0	1.5

Pitch and Yaw Angular Rates of a Rocket after Launcher Exit

Pitch and yaw angular rates of a rocket $\tilde{q}$ and $\tilde{r}$ are the projections of the angular rate vector $\boldsymbol{\omega}$ to the $O\tilde{z}$ and $O\tilde{y}$ axes of the aero ballistic reference frame. Considering the linearized model of the rocket atmospheric flight in the vertical plane under the influence of gravity [20], and transforming the differential equations of motion from the body to the aero-ballistic reference frame, we have:

$$\begin{aligned} \Delta\dot{\tilde{w}} &= z_w(t)\Delta\tilde{w} + u(t)\Delta\tilde{q} + g\cos\Theta(t) \\ \Delta\dot{\tilde{q}} &= m_w(t)\Delta\tilde{w} + m_q(t)\Delta\tilde{q} \end{aligned} \tag{1}$$

The dynamic coefficients in equation (1), z_w, m_w, m_q are dependent on the rocket velocity $u(t)$, its inertial characteristics and the atmosphere. Since the action of the Active damping control system occurs during the burst phase, the values of velocity, mass and CG location of the rocket change significantly during time, and these parameters are assumed as time-varying. For a specified reference trajectory and the corresponding aerodynamic parameters values, in a moment in the time τ, we have:

$$\Delta\ddot{\tilde{q}} + 2\zeta_n(\tau)\omega_n(\tau)\Delta\dot{\tilde{q}} + \omega_n^2(\tau)\Delta\tilde{q} = m_w(\tau)g\cos\Theta(\tau) \tag{2}$$

Neglecting the oscillatory transient process, the steady state value of the pitch rate is:

$$\tilde{q}_R = \frac{m_w}{\omega_n^2} g\cos\Theta \tag{3}$$

Fig.1 shows the comparison of the pitch rate steady state values obtained by equation (3) and the pitch rate values obtained by the simulation of the 6-DOF model. After the launcher tube exit, the rocket pitch rate is significantly higher than its steady state (reference) value, which produces the oscillatory transient process. After the transient process is over, the pitch rate settles at its steady state value.

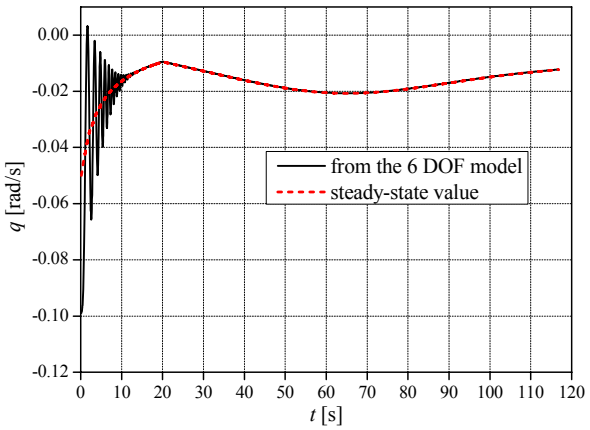

Figure 1. The pitch rate and its reference value.

In the horizontal plane, without gravity influence, the yaw rate steady state value is $\tilde{r}_R = 0$. In the ideal case, the active damping control system should suppress the oscillations of the transient process after the launcher exit, and achieve $\tilde{q}(t) = \tilde{q}_R(t)$ and $\tilde{r}(t) = 0$. For that to be possible, one should have to know the values of the pitch and yaw rates in the aero-ballistic frame. Considering the fact that the rate gyros are fixed to the rocket body and measure the values of q, r in the body reference frame, the determination of $\tilde{q}$ and $\tilde{r}$ requires the value of the roll angle Φ, which could be obtained by the integration of the output of another rate gyro, measuring the roll rate p, which should be of a high accuracy class. The further study shows that the correction can be done with the pitch and yaw rate values in the body reference frame, thus significantly simplifying the control system. Furthermore, these sensors could be of a low accuracy class, as they are not intended for obtaining the rocket's Euler angles via their output integration.

Denoting the transformation matrix from the body to the aero-ballistic frame with $L_{\tilde{B}B}$ (Etkin, Reid [20]), for a known roll angle Φ, the angular rate vector components in the aero-ballistic frame are:

$$\tilde{\boldsymbol{\omega}} = \begin{bmatrix} \tilde{p} \\ \tilde{q} \\ \tilde{r} \end{bmatrix} = \mathbf{L}_{\tilde{B}B}\boldsymbol{\omega} = \begin{bmatrix} 1 & 0 & 0 \\ 0 & \cos\Phi & -\sin\Phi \\ 0 & \sin\Phi & \cos\Phi \end{bmatrix} \begin{bmatrix} p \\ q \\ r \end{bmatrix} \tag{4}$$

In the considered study case, the design of the rocket and the launcher tube allows that the roll rate is significantly (3-5 times) higher than the pitch rate natural frequency. Thus, the body fixed rate gyros readings are oscillatory with the roll rate frequency. If the angular rate vector $\boldsymbol{\omega} = [p \quad q \quad r]^T$ is considered, then its projection to the Cyz plane is $\boldsymbol{\omega}_{yz} = [0 \quad q \quad r]^T$. In the aero-ballistic frame, we have: $\tilde{\boldsymbol{\omega}} = [\tilde{p} \quad \tilde{q} \quad \tilde{r}]^T$ and its projection to the plane $C\tilde{y}\tilde{z}$: $\tilde{\boldsymbol{\omega}}_{yz} = [0 \quad \tilde{q} \quad \tilde{r}]^T$. The amplitude of the vector $\boldsymbol{\omega}_{yz}$ and its angle in the plane Cyz in relation to the y axis are:

$$\omega_{yz} = \sqrt{q^2 + r^2} \tag{5}$$

$$\Phi_\omega = \tan^{-1}\frac{r}{q} \tag{6}$$

Fig.2 shows the pitch and yaw rates in the body and the aero-ballistic frame, as well as the amplitude of the angular rate vector in the Cyz plane during the first 10 seconds after the launch. While the values of $\tilde{q}$ oscillate around the reference value given by equation (3), and the values of $\tilde{r}$ around zero, with the pitch rate natural frequency, the angular rates in the body reference frame oscillate with the roll rate frequency. However, the amplitude of the angular rate vector ω_{yz}, obtained from the values of q and r, oscillates not with the roll rate, but with the pitch rate natural frequency around the absolute value of the pitch rate reference value $\tilde{q}_R$.

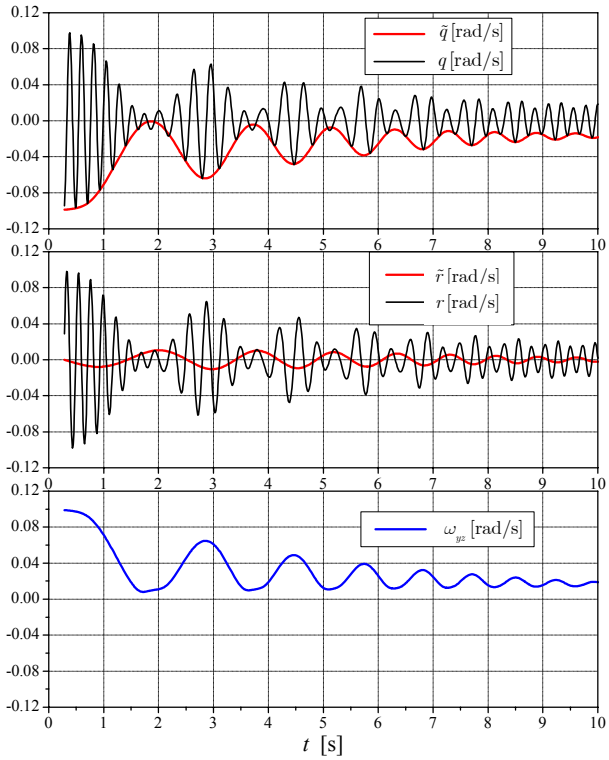

Figure 2. Pitch and yaw rates.

As seen in Fig.1, after the launcher exit, the rocket angular rates oscillate provoking the oscillations of the pitch and yaw angle as well as the angle of attack and sideslip. The character of the transient process (Fig.1) implicates that the transversal motion of the rocket is very oscillatory, with a very low damping ratio. The task of the active damping control system is to increase the damping ratio and to suppress the oscillations. If the control angular acceleration in the body reference frame is denoted with $\dot{\boldsymbol{\omega}}_c$, the active damping control law is:

$$\dot{\boldsymbol{\omega}}_c = -K_\omega \boldsymbol{\omega}_{yz}, \quad K_\omega > 0 \tag{7}$$

Transforming the previous equation into the aero-ballistic reference frame, we obtain:

$$\dot{\tilde{\boldsymbol{\omega}}}_c = \mathbf{L}_{\tilde{B}B}\dot{\boldsymbol{\omega}}_c = -K_\omega \mathbf{L}_{\tilde{B}B}\boldsymbol{\omega}_{yz} = -K_\omega \mathbf{L}_{\tilde{B}B}\mathbf{L}_{B\tilde{B}}\tilde{\boldsymbol{\omega}}_{yz} = -K_\omega \tilde{\boldsymbol{\omega}}_{yz} \tag{8}$$

The scalar form of the previous equation is:

$$\begin{aligned} \dot{\tilde{q}}_c &= -K_\omega \tilde{q} \\ \dot{\tilde{r}}_c &= -K_\omega \tilde{r} \end{aligned} \tag{9}$$

System (1) now becomes:

$$\begin{aligned} \Delta\dot{\tilde{w}} &= z_w(t)\Delta\tilde{w} + u(t)\Delta\tilde{q} + g\cos\Theta(t) \\ \Delta\dot{\tilde{q}} &= m_w(t)\Delta\tilde{w} + [m_q(t) - K_\omega]\Delta\tilde{q} \end{aligned} \tag{10}$$

This system of differential equations can be transformed into:

$$\begin{aligned} &\Delta\ddot{\tilde{q}} + 2\zeta_{n\,\mathrm{AD}}(\tau)\omega_{n\,\mathrm{AD}}(\tau)\Delta\dot{\tilde{q}} + \omega^2_{n\,\mathrm{AD}}(\tau)\Delta\tilde{q} = \\ &= m_w(\tau)\, g\cos\Theta(\tau) \end{aligned} \tag{11}$$

The system described by the previous differential equation achieves the steady state:

$$\tilde{q}_{R\,\mathrm{AD}} = \frac{m_w}{\omega^2_{n\,\mathrm{AD}}} g\cos\Theta, \tag{12}$$

the value of which is very close to the steady state value in the case without the active damping, given by equation (3). Introducing $m_{q\,\mathrm{AD}} = m_q - K_\omega$, the natural frequency and the damping ratio become:

$$w^2_{n\mathrm{AD}} = m_{q\,\mathrm{AD}} z_w - m_w V \tag{13}$$

$$\zeta_{n\,\mathrm{AD}} = \frac{-z_w - m_{q\,\mathrm{AD}}}{2\omega_n} \tag{14}$$

From the previous equations, we obtain:

$$\begin{aligned} m_{q\,\mathrm{AD}} = &(2\zeta_{n\,\mathrm{AD}} - 1) z_w - \\ &-2\sqrt{\zeta_{n\,\mathrm{AD}}(\zeta_{n\,\mathrm{AD}} - 1) z_w^2 - \zeta_{n\,\mathrm{AD}} m_w V} \end{aligned} \tag{15}$$

which, for the assumed value of $\zeta_{n\mathrm{AD}} = 1$ comes to $m_{q\,\mathrm{AD}} = z_w - 2\sqrt{-m_w V}$. Fig.3 shows the values of $m_{q\,\mathrm{AD}}$ obtained for $\zeta_n = 1$, during the first 10 seconds of flight after the launch.

From Fig.3, assuming that $\zeta_{n\mathrm{AD}} = 1$, we have $K_\omega \approx -m_{q\,\mathrm{AD}} \approx 18\,\mathrm{s}^{-1}$. The comparison of the natural frequencies and the damping ratios in the cases without control and with active damping with $K_\omega = 18\,\mathrm{s}^{-1}$ for the first 10 s after launch is shown in Fig.4.

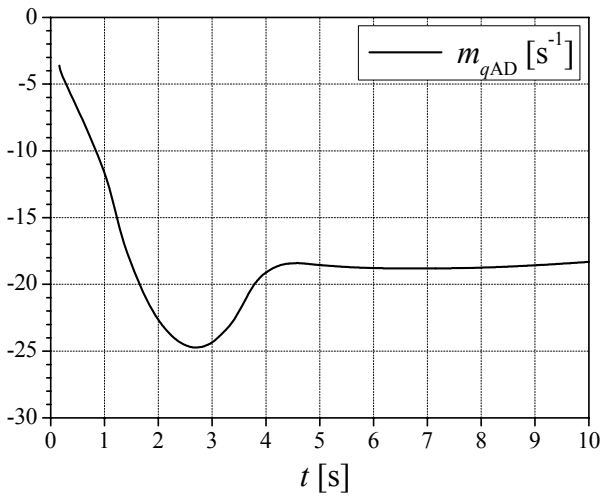

Figure 3. Values of $m_{q\,\mathrm{AD}}$ for $\zeta_n = 1$.

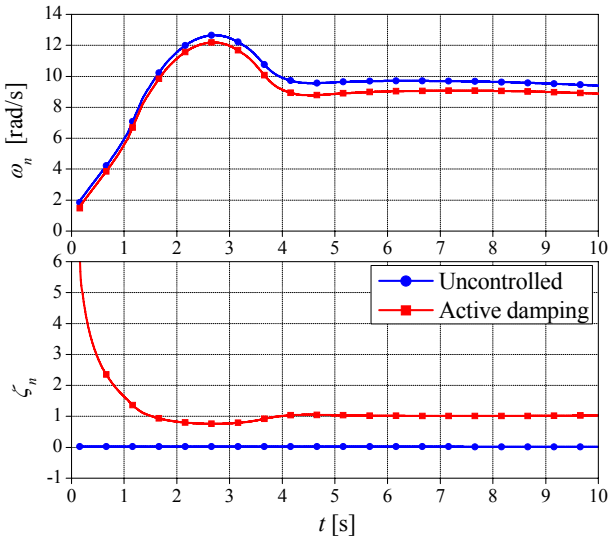

Figure 4. Influence of active damping on the values of ζ_n and ω_n.

Fig.4 shows that active damping slightly lowers the system dynamics and increases the damping ratio from the near-zero value to the desired $\zeta_n = 1$.

Pulse Frequency Modulation of the Command Signal

Equations (5 - 7) describe the active damping control law. Continuous control command (7) must be transformed into an array of pulses, using pulse frequency modulation, as described in [5]. The action of a control impulse with magnitude $I_c\,[\mathrm{N\text{-}s}]$ at a distance $l_I\,[\mathrm{m}]$ from the center of gravity of the rocket with the pitch inertia $J_y\,[\mathrm{kg\text{-}m^2}]$, produces an angular acceleration, whose mean value $\dot{\hat{\omega}}_c$ over the preceding period $\tau\,[\mathrm{s}]$ is:

$$\dot{\hat{\omega}}_c = \frac{I_c l_I}{\tau J_y} \tag{16}$$

The mean value of the angular acceleration depends on the only variable member of equation (16) – the time period τ. The maximum value of the angular acceleration, $\dot{\hat{\omega}}_{c,\max}$ corresponds to the minimum time between two consecutive pulses $t_{\min}$. By defining the command coefficient K as the ratio between the achieved and the maximum angular acceleration, we obtain:

$$K = \frac{\left|\dot{\hat{\omega}}_c\right|}{\dot{\hat{\omega}}_{c,\max}} \tag{17}$$

For $\dot{\hat{\omega}}_c$ defined by equation (7), and $\dot{\hat{\omega}}_{c,\max}$ defined by (16) with $\tau = t_{\min}$, we have:

$$K = \frac{t_{\min} J_y K_\omega}{I_c l_I}\omega_{yz} = K_P \omega_{yz} \tag{18}$$

$$K_P = \frac{t_{\min} J_y K_\omega}{I_c l_I}\ [\mathrm{s}] \tag{19}$$

The gain K_P depends on the angular rate feedback gain K_ω and the parameters of the pulse frequency modulation. For a specified magnitude of control pulses, their distance from the c.g. of the rocket and its inertial characteristics, the value of the gain K_P is defined by $t_{\min}$ and K_ω.

The pulse frequency modulation of the control signal ($\dot{\boldsymbol{\omega}}_c$) requires the application of a non-linear control law instead of equation (7) in order to avoid oscillations around zero, which comes with the impulse control. Therefore, the control action, defined with equation (7), stops when the magnitude of ω_{yz} falls below a given value ω_{dem}. The control law, then, becomes:

$$K = \begin{cases} K_P\left(\omega_{\mathrm{dem}} - \omega_{yz}\right) & ,\ \omega_{\mathrm{dem}} < \omega_{yz} \\ 0 & ,\ \omega_{\mathrm{dem}} \geq \omega_{yz} \end{cases} \tag{20}$$

The command coefficient values, representing the ratio between the desired and the maximum possible angular acceleration are limited to $K \leq 1$. The time to the next pulse is defined as:

$$\tau = \frac{t_{\min}}{K}, \tag{21}$$

A block diagram of the active damping control system is shown in Fig.5.

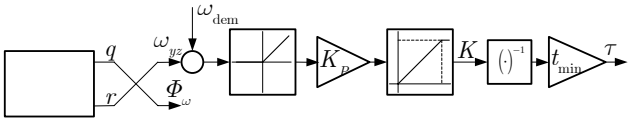

Figure 5. Block diagram of the active damping control system.

The conditions for firing the n-th pulsejet are:

- Time elapsed from the previous pulse is longer than τ: $t > t_{\mathrm{prev}} + \tau$.
- Considered n-th pulsejet is not already fired.
- Difference between its roll angle and the desired one, taking into account the equivalent delay angle Φ_d, is lower than the desired activation threshold ε_Φ:

$$\left|\Delta\Phi_n + \Phi_d - \Phi_\omega\right| < \varepsilon_\Phi \tag{22}$$

The angular condition, given by equation (22) is shown in Fig.6. The term $\Delta\Phi_n = 2\pi(n-1)/N_I$ presents the roll

angle of the n-th pulsejet measured from the negative part of the z axis in the body reference frame. The roll angle Φ_ω of the angular velocity vector projection $\boldsymbol{\omega}_{yz}$ onto the plane Cyz of the body reference frame is defined by equation (6) in respect to the y axis. The control angular acceleration vector $\dot{\boldsymbol{\omega}}_c$, is, according to equation (7), opposite to $\boldsymbol{\omega}_{yz}$. The control impulse vector $\mathbf{I}_c$ is in a plane normal to the vector $\dot{\boldsymbol{\omega}}_c$. All these vectors lie in, or are parallel to, the plane Cyz. Fig.6 shows that the angle between the y axis and the vector $\boldsymbol{\omega}_{yz}$, and the angle between the negative part of the z axis and the projection of the vector $\mathbf{I}_c$ are equal (to Φ_ω), being the angles with normal arms. This proves (22).

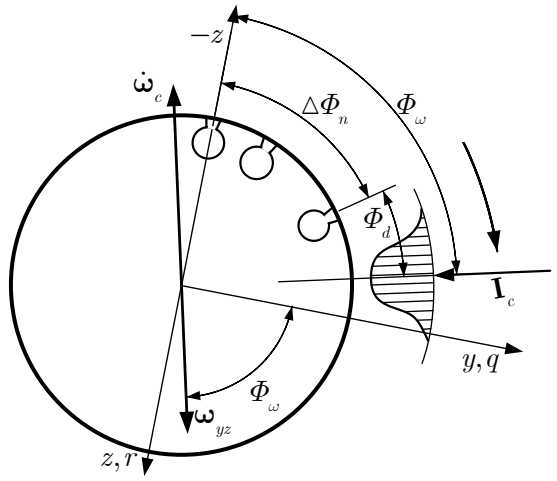

Figure 6. Pulse command roll angle.

The equivalent roll angle Φ_d is dependent on the roll rate, the firing time delay and the duration of the pulse τ_I. Without the roll rate sensor, the value of p is assumed as a known function of the time of flight.

Simulation results

The active damping system action is shown for a combination of disturbances given in Table 2. It is assumed that the control system consists of $N_I = 32$ pulsejets with a magnitude of $I_c = 15\,\text{N-s}$, as well as that the control law parameters are: $K_P = 20\,\text{s}$, $\omega_{\text{dem}} = 0.01\,\text{rad/s}$ and $t_{\min} = 0.1\,\text{s}$.

Table 2.

Quantity	Unit	Nominal value	Disturbed value
$\tilde{q}_0$	rad/s	-0.099	-0.14
$\tilde{r}_0$	rad/s	0	-0.02
V_{Wx}	m/s	0	-2
V_{Wy}	m/s	0	2
ε	mrad	0	1.5

Figs.7 and 8 show the comparison of the pitch and yaw rates in the aero-ballistic frame for rockets with active damping and without any control. An active damping system, using the array of control pulses, efficiently suppresses oscillations in the horizontal plane and maintains the yaw rate close to zero.

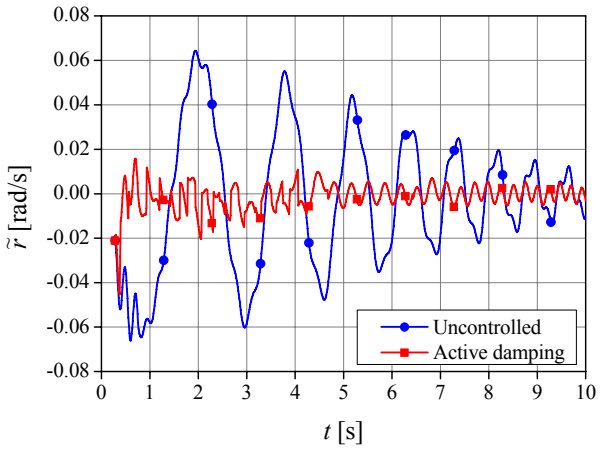

Figure 7. Yaw rates with and without the control system.

The situation in the vertical plane is somewhat different. After the launcher exit, the control system sets the pitch rate to a near zero value. With the oscillations suppressed, the angle of attack increases, as shown in Fig.9. This low value of the pitch rate is, also, in collision with the steady state value, given by equation (3) and shown on Fig.1, whose value after the launch is around $\tilde{q}_R \approx 0.04\,\text{rad/s}$. The previous two facts are the reason for a large number of control pulses fired in an attempt to maintain the pitch rate within the given boundaries. Figs. 7 and 8 show that the roll angles of the command pulses were close to the vertical plane, besides the fact that the control logic was performed in the body reference frame, without the information about the roll angle.

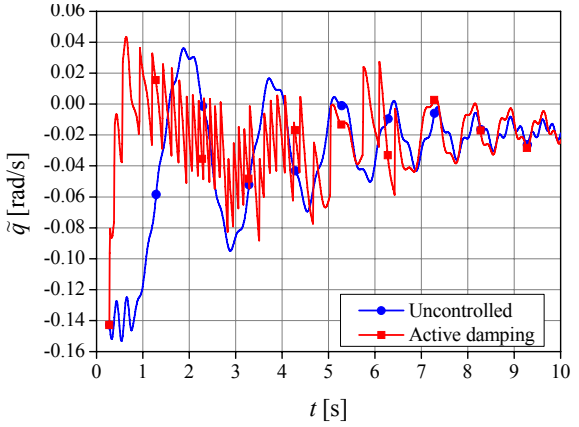

Figure 8. Pitch rates with and without the control system.

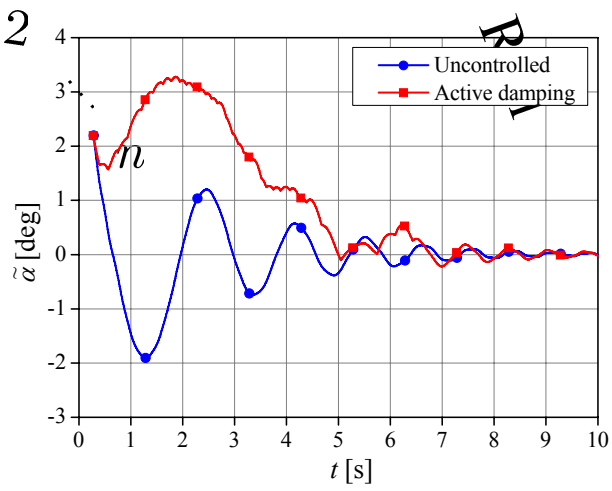

Figure 9. Angle of attack $\tilde{\alpha}$, with and without the control system.

Fig.10 shows the magnitude of the angular rate vector in the transversal plane ω_{yz}, defined by equation (5), which, in this case, is the controlled state. The control system firing moments are shown as well. After all the pulses were expended at time t = 6.5 s, free oscillations of the angular rate ω_{yz} occur. The amplitude of these oscillations in the vertical plane is similar to the amplitude of the uncontrolled rocket, due to the difference between the actual and steady-state value of the pitch rate $\tilde{q}$. The oscillations in the horizontal plane remain suppressed even after the control stops, with only low-amplitude roll rate frequency oscillations remaining due to the rocket motor thrust misalignment.

Figs. 11 and 12 show the comparison of the yaw and pitch angles during the transient process after the launcher exit. The cases with and without disturbances given in Table 2, and the cases with and without the control are shown in order to present the effect of the control system. Although the active damping control system was not able to compensate the effect of the disturbances completely, it manages to lower significantly the difference between the pitch and yaw angles in the case with and without disturbances. From the yaw angle diagram, one can note that the difference is lowered from 2.6° to 1.2°. In the pitch angle case, the difference reduction due to the active damping control system action is somewhat lower, from 1.9° to 1.2°.

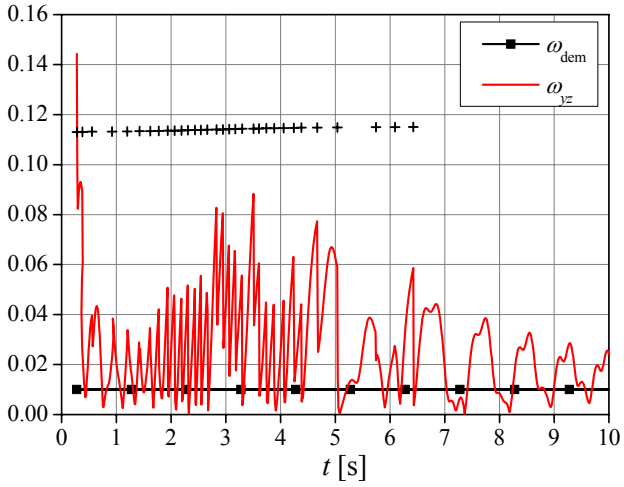

Figure 10. The demanded and the achieved angular rates.

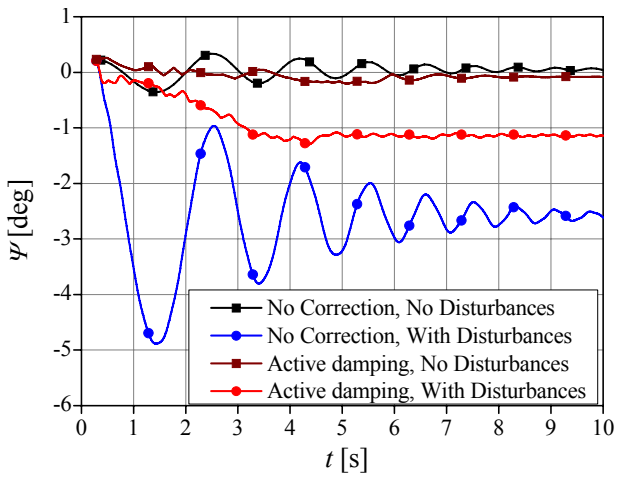

Figure 11. Yaw angles comparison.

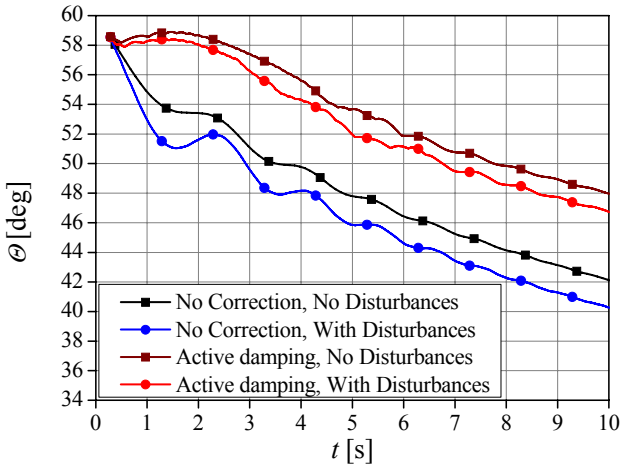

Figure 12. Pitch angles comparison.

Parametric and Performance Analysis

The goal of the parametric analysis is to determine the optimal control system parameter values corresponding to its hit point deviation. The analysis is performed using the Monte Carlo method, described in [21], with 200 simulations of the 6-DOF model. The mean values and the standard deviations of the stochastic parameters are given in Table 1.

Hit Points Distribution

Fig.13 shows the hit point distribution using the Monte Carlo method. The cases of the uncontrolled rockets as well as of the rockets with the active damping control system, with the parameters $I_c = 15\,\text{N-s}$, $N_I = 32$, $t_{\min} = 0.1\,\text{s}$, $\omega_{\text{dem}} = 0.01\,\text{rad/s}$ and $K_P = 20\,\text{s}$, are shown. It was assumed that all control pulses lasted for $\tau_I = 0.005\,\text{s}$. The analysis was performed for a statistical sample of 200 simulations.

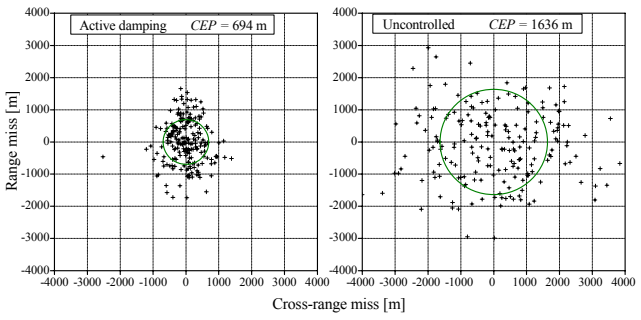

Figure 13. Hit point distribution.

The statistics of the hit point distributions is shown in Table 3.

Table 3.

Statistics	Uncontrolled	Active damping	Reduction ratio
Circular error probable CEP[m]	1636	694	2.36
Range error probable V_D[m]	741	466	1.59
Lateral error probable V_P[m]	1094	321	3.41

Using the active damping control system, dispersion is lowered by a factor of 3.4 in the cross-range, and by a

factor of 1.5 in the range. The inability of such a control system to compensate for the total impulse deviation changes the character of the hit point distribution, and the dispersion in the range becomes greater than that in the cross-range.

Active guidance control system parametric analysis

The performances of the precision enhancement system depend on its parameters, which are: the number N_I and the magnitude I_c of the pulse jets, the minimum time between two consecutive pulses $t_{\min}$, the gain factor K_P, the demanded angular rate ω_{dem} and the average duration of control pulses τ_I. The parameter tuning method is used for their optimal combination, which yields the least impact point dispersion.

Fig.14 shows the dependence of the impact point dispersion on the combination of the gain factor K_P and $t_{\min}$. In the considered case, the other parameters were: $N_I = 32$, $I_c = 15\,\text{N-s}$, $\omega_{\text{dem}} = 0.01\,\text{rad/s}$ and $\tau_I = 0.005\,\text{s}$.

The parameters K_P and $t_{\min}$ are linked in equation (19). For the assumed damping ratio $\zeta_n = 1$, which, according to equation (15) yields $K_\omega \approx -m_{qAD} \approx 19\,\text{s}^{-1}$, and for the parameters $J_y = 562\,\text{kg-m}^2$ and $l_I = 2.44\,\text{m}$, from equation (19), we have $K_P = 276 \cdot t_{\min}$.

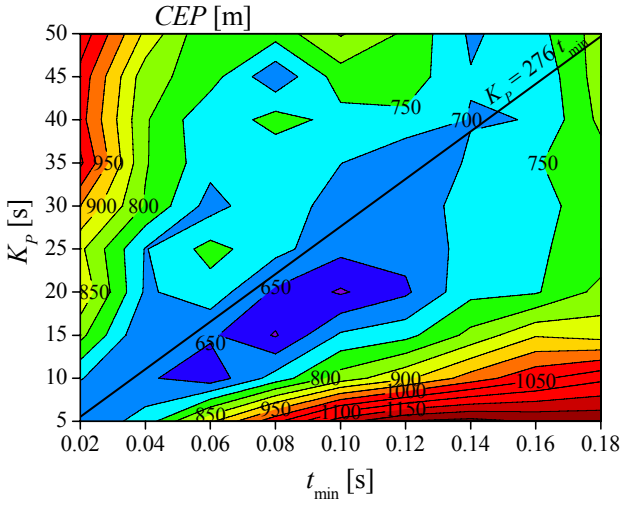

Figure 14. *CEP* depending on K_P and $t_{\min}$.

The dependence of the hit points distribution on the parameters K_P and $t_{\min}$ shown in Fig. 14 leads to the conclusion that the assumed value of $\zeta_n = 1$ is close to the optimum one. The best results area is clearly differentiated in Fig.14 and close to the line $K_P = 276 \cdot t_{\min}$. The specific character of the applied pulse control favors a certain range of the minimum time between two pulses, and we can assume the values $t_{\min} = 0.1\,\text{s}$ and $K_P = 20\,\text{s}$ for a further analysis.

Fig.15 shows the dependence of hit point dispersion on the demanded angular rate ω_{dem}. For a given magnitude of $I_c = 15\,\text{N-s}$ and various numbers of control pulses, series of Monte Carlo simulations were performed for $\tau_I = 0.005\,\text{s}$ and all combinations of K_P and $t_{\min}$, and the least achieved dispersions are shown. This analysis shows that the dispersion is only slightly dependent on ω_{dem}. In the case of an extremely low number of control pulses, better results are obtained for higher values of ω_{dem}, while, with the increase of the pulsejets number, the value that yields the least impact point dispersion becomes $\omega_{\text{dem}} = 0.01\,\text{rad/s}$.

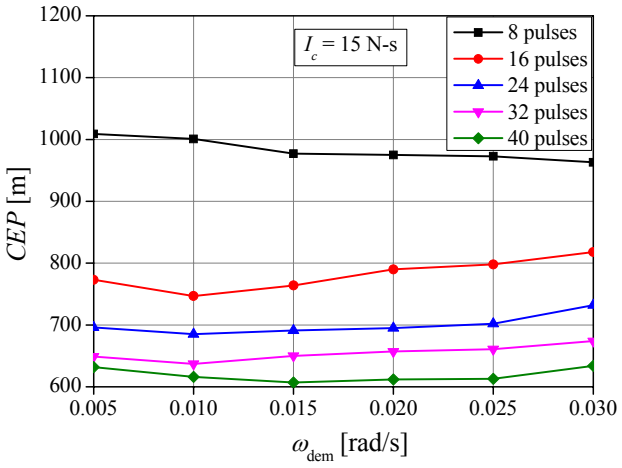

Figure 15. *CEP* depending on ω_{dem}.

Fig.16 shows the dependence of the impact point dispersion on the pulse duration τ_I, for the case of 32 pulsejets with a magnitude of $I_c = 15\,\text{N-s}$ and the combination of software parameters which, according to the previous analysis, yields the best results for such energy resources. This analysis shows the negative impact of the pulse duration on the impact point dispersion, and that this parameter should be lowered as much as possible in the design of the control system.

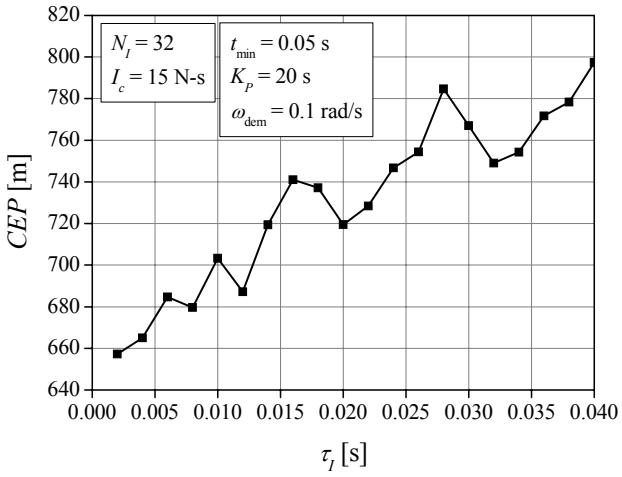

Figure 16. *CEP* depending on the control pulse duration.

Fig.17 presents the overall performances of the active damping control system in relation to its energy resources – number and magnitude of the pulsejets. Each point on the diagram is obtained for the combination of the control parameters which yields the least impact point dispersion and $\tau_I = 0.005\,\text{s}$. This analysis shows that $I_c = 20\,\text{N-s}$ yields the best results. The dispersion reduces significantly with the number of pulsejets increase to 16. In the case of high magnitude pulses, the increase of their number above this value produces a low or none dispersion reduction, In the case of low intensity pulses, any increase of their

number lowers the dispersion significantly, which implies that in this case the control system is energy-limited.

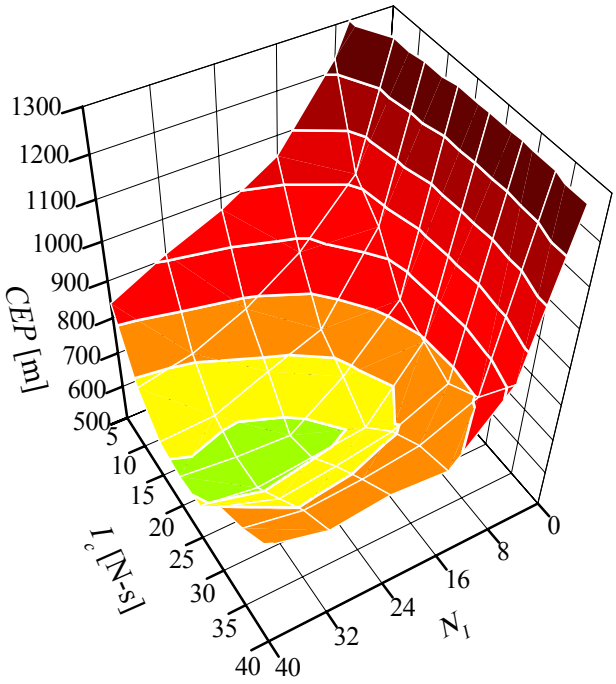

Figure 17. *CEP* depending on the control system energy resource.

Conclusion

The problem of impact point dispersion comes as a limitation factor for artillery rockets uses at ranges greater than 30 km, in which case a very large number of rockets are needed for achieving a hit points concentration which guarantees the target destruction. The number of rockets can be reduced by improving their precision which can be achieved by the implementation of a control system.

Considering the fact that artillery rockets are used for firing at entire areas, which implicates that they are launched in large quantities from multi-tube launchers, the cost of the applied control system in relation to its precision enhancing is of great importance. A significant reduction of the price and complexity of the control system can be achieved using pulsejets as a control mechanism.

This paper presents a precision enhancing method named the active damping method. This control system provides correction of the disturbances on the critical part of the trajectory, immediately after the launcher tube exit. Such a control system is significantly simpler and cheaper than trajectory tracking systems, as it demands only two rate gyros of a low accuracy class.

This paper presents the parametric and performance analysis of the active damping control system. It is shown that such a system can lower the circular error probable by a factor of 2.5. The active damping control system, with its simplicity and performance, is a strong candidate for the use on 128/122 mm artillery rockets.

References

[1] HARKINS,T., BROWN,T.: Using Active Damping as a Precision-Enhancing Technology for 2.75-inch Rockets, ARL-TR-1772, U.S. Army Research Laboratory, Aberdeen Proving Ground, MD, 1999.

[2] JITPRAPHAI,T., COSTELLO,M.: *Dispersion Reduction of a Direct Fire Rocket Using Lateral Pulse Jets*, Journal of Spacecraft and Rockets, 2001, Vol.38, No.6, pp.929-936.

[3] JITPRAPHAI,T., BURCHETT,B., COSTELLO,M.: *A Comparison of Different Guidance Schemes for a Direct-fire Rocket with a Pulse Jet Control Mechanism*, U.S. Army Research Lab, ARL-CR-493, Aberdeen Proving Ground, MD, April 2002.

[4] GUPTA,S.K., SAXENA,S., SINGHAL,A., GHOSH,A.K., *Trajectory Correction Flight Control System using Pulsejet on an Artillery Rocket* Defense Science Journal, 2008, Vol.58, No.1, pp.15-33.

[5] PAVKOVIĆ, B., PAVIĆ, M., ĆUK, D., "Trajectory Correction of Artillery Rockets using Trajectory Tracking with Pulse Frequency Modulation", 4th International Scientific Conference on Defensive Technologies OTEH 2011 Proceedings, Belgrade 2011, pp 211-216..

[6] ČUK,D., PAVIĆ,M., PAVKOVIĆ,B.: *Comparison of Different Guidance Laws for a Mortar Missile With a Pulse Jet Control Mechanism*, 4th International Scientific Conference on Defensive Technologies OTEH 2011 Proceedings, Belgrade 2011, pp.217-223.

[7] AMITAY,M., SMITH,D., KIBENS,V., PAREKH,D., GLEZER,A.: *Aerodynamic Flow Control over an Uncon ventional Airfoil Using Synthetic Jet Actuators*, AIAA Journal, 2001,Vol.39, No.3, pp.361-370.

[8] HARKINS,T., DAVIS,B., Drag-Brake Deployment Method and Apparatus for Range Error Correction of Spinning, Gun-Launched Artillery Projectiles," U.S. Patent 6345785, issued 12 Feb. 2002.

[9] HILLSTROM,T., OSBORNE,P.: *United Defense Course Correcting Fuze for the Precision Guidance Kit Program*, 49th Annual Fuze Conference, National Defense Industrial Association, Arlington, Apr. 2005,VA, 5–7.

[10] MASSEY,K., FLICK,A.: *Mechanical and Jet Actuators for Guiding a Small Caliber Subsonic Projectile*, 25th AIAA Applied Aerodynamics Conference, Miami, FL, AIAA Paper 2007-3813, 25–28 June 2007.

[11] MASSEY,K., MCMICHAEL,J., WARNOCK,T., HAY,F.: *Mechanical Actuators for Guidance of a Supersonic Projectile*, 23rd AIAA Applied Aerodynamics Conference, Toronto, Ontario, Canada, AIAA June 2005, 6–9, pp.2005-4970,.

[12] COSTELLO,M., AGARWALLA,R.: *Improved Dispersion of a Fin Stabilized Projectile Using a Passive Moveable Nose*, Journal of Guidance, Control, and Dynamics, 2000, Vol.23, No.5, pp.900-903.

[13] COSTELLO,M.: *Extended Range of a Gun Launched Smart Projectile Using Controllable Canards*, Shock and Vibration, 2001, Vol.8, No.3-4, pp.203–213.

[14] COSTELLO,M., PETERSON,A.: *Linear Theory of a Dual Spin Projectile in Atmospheric Flight*, Journal of Guidance, Control, and Dynamics, 2000, Vol.23, No.5, pp.789-797.

[15] BURCHETT,B., PETERSON,A., COSTELLO,M.: *Prediction of Swerving Motion of a Dual-Spin Projectile with Lateral Pulse Jets in Atmospheric Flight*, Mathematical and Computer Modeling, 2002, Vol.35, No.7-8, pp.821–834.

[16] CHANDGADKAR,S., COSTELLO,M., DANO,B., LIBURDY,J., PENCE,D.: *Performance of a Smart Direct Fire Projectile Using a Ram Air Control Mechanism*, Journal of Dynamic Systems, Measurement, and Control, 2002, Vol.124, No.4, pp.606–612.

[17] ROGERS,J., COSTELLO,M.: *Control Authority of a Projectile Equipped with an Internal Translating Mass*, 2007 AIAA Atmospheric Flight Mechanics Conference, Hilton Head, SC, AIAA 2007, pp.2007-6492.

[18] MANDIĆ,S.: *Guidance of Ground to Ground Rockets Using Flight Path Steering Method*, Scientific Technical Review, ISSN 1820-0206, 2009, Vol.59, No.3-4, pp.3-11.

[19] GANTMAKHER,F.R. LEVIN,L.M.: *The Flight of Uncontrolled Rockets*, Pergamon Press, 1964.

[20] ETKIN,B., REID,L.D.: *Dynamics of Flight*, Stability and Control, John Wiley & Sons, 1995, pp.93-160.

[21] TAYLOR,J.H., PRICE,C.F.: *Direct Statistical analysis of Missile Guidance Systems via CADETTM*, The Analytic Sciences Corporation, 1975.

Received: 18.04.2012.

Povećanje preciznosti artiljerijskih raketa metodom aktivnog prigušenja

Artiljerijske rakete srednjeg i velikog dometa se koriste na bojištu za indirektno gađanje udaljenih ciljeva. Imajući na umu veliko rasturanje pogodaka, one se koriste za gađanje celih oblasti iz višecevnih lansera. Pri tome, za ostvarivanje zahtevane verovatnoće neutralizacije pretnje, neophodno je utrošiti veliki broj raketa. Primenom odgovarajućeg upravljačkog sistema kod artiljerijskih raketa moguće je znatno smanjiti njihovo rasturanje pogodaka i povećati verovatnoću uništenja ciljeva. Upravljački sistemi sa reaktivnim impulsima su dovoljno jednostavni da se mogu primeniti na artiljerijskim raketama i efikasni da ostvare smanjenje rasturanja pogodaka koje opravdava njihovu primenu. U ovom radu je predstavljena pojednostavljena upravljačka šema nazvana metoda aktivnog prigušenja, koja izvršava korekciju poremećaja odmah nakon napuštanja lansirne cevi. Pokazano je da se primenom upravljačkog sistema sa aktivnim prigušenjem može ostvariti značajno smanjenje rasturanja pogodaka, kao i da je to efikasan metod za smanjenje uticaja svih poremećaja izuzev odstupanja vrednosti totalnog impulsa raketnog motora.

Ključne reči: **raketna artiljerija, višecevni raketni bacač, raketni projektil, upravljanje raketom, vođenje rakete, sistem za upravljanje, impulsno upravljanje, preciznost, korekcija greške, rasturanje pogodaka, efekti na cilju, Metoda Monte Karlo.**

Увеличение точности артиллерийских ракет с использованием активного демпфирования

Артиллерийские ракеты средней и большой дальности пользуются на поле боя для косвенной съёмки отдалённых объектов. Принимая во внимание широкое распределение хитов, они привыкли снимать всю область из пусковых установок с выше труб. Кроме того, для достижения требуемой вероятности нейтрализации угрозы, необходимо потреблять большое количество ракет. Используя соответствующие системы для управления у артиллерийских ракет возможно значительно снизить распределения своих хитов и увеличить вероятность поражения целей. Системы для управления с реактивными импульсами достаточно просты для применения на артиллерийских ракетах и для достижения эффективного снижения распределения хитов, которые оправдывают их применение. Эта статья представляет собой упрощенную схему для управления с названием - метод активного демпфирования, который выполняет коррекцию нарушений сразу после окончания запуска трубы пусковой установки. Показано, что с применением системы для управления с активным демпфированием можно добиться значительного сокращения точек распределение хитов, а также что это является эффективным методом для снижения воздействия всех нарушений, за исключением отклонений от общего числа импульсов ракетных двигателей.

Ключевые слова: **реактивная артиллерия, реактивная система залпового огня, ракетные ракеты, управления ракетой, наведения ракет, системы для управления, импульсное управление, точность, исправление ошибок, распределение хитов, воздействие на цель, метод Монте-Карло.**

L’augmentation de la précision chez les roquettes d’artillerie par la méthode d’étouffement actif

Les roquettes d’artillerie de moyenne et de grande portée sont utilisées sur le champ de bataille pour les tirs indirects sur les objets éloignés. Tenant compte de la grande dispersion des impacts elles sont utilisées pour tirer sur les entières régions à partir des lanceurs multitubes. Pour réaliser la probabilité exigeante de la neutralisation de menace il est nécessaire de dépenser un grand nombre de roquettes. En utilisant un système de contrôle correspondant chez les roquettes d’artillerie il est possible de diminuer considérablement la dispersion des impacts et d’augmenter la possibilité de destruction des objectifs. Les systèmes de contrôle aux impulsions réactives sont assez simples pour s’appliquer chez les roquettes d’artillerie et suffisamment efficaces pour diminuer la dispersion ce qui justifie leur emploi. Dans ce travail on a présenté le schéma simplifié de contrôle appelé la méthode d’étouffement actif qui accomplit la correction du dérangement immédiatement après l’abandon du tube de lancement. On a démontré que par l’emploi du système de contrôle à l’étouffement actif il est possible de réaliser une diminution considérable de la dispersion et que cette méthode est efficace pour diminuer les effets de tous les dérangements sauf la déviation de l’impulsion totale chez le moteur de la roquette.

Mots clés: **artillerie de roquettes, lanceur de roquettes multitube, missile, contrôle de roquette, guidage de roquette, système de contrôle, contrôle par impulsion, précision, correction de déviation, dispersion, effets sur l’objectif, méthode Monté Carlo.**